Rare Earth Elements in early-diagenetic foraminifer 'coatings': Pore-water controls and potential palaeoceanographic applications

L. C. Skinner, A. Sadekov, Margaux Brandon, M. Greaves, Y. Plancherel, M. de la Fuente, J. Gottschalk, S. Souanef-Ureta, D. S. Sevilgen, A. E. Scrivner

Rare Earth Elements in early-diagenetic foraminifer 'coatings': pore-water controls and potential palaeoceanographic applications

L.C. Skinner*[1], A. Sadekov[2], M. Brandon[3], M.Greaves[1], Y. Plancherel[4], M. de la Fuente[1], J. Gottschalk[5], S. Souanef-Ureta[1], D.S. Sevilgen[6], A.E. Scrivner[1]

*Corresponding author. Tel. +44 1223 333406

E-mail address: luke00@esc.cam.ac.uk (L. Skinner)

1. Godwin Laboratory for Palaeoclimate Research, Department of Earth Sciences, University of Cambridge, Downing Street, Cambridge, CB2 3EQ, United Kingdom.
2. ARC Centre of Excellence for Coral Reef Studies, School of Earth Sciences, University of Western Australia, 35 Stirling Highway, Crawley, WA, 6009.
3. GEOPS, Univ. Paris-Sud, CNRS, Université Paris-Saclay, Rue du Belvédère, Bât. 504, 91405 Orsay, France.
4. University of Oxford, Department of Earth Sciences, South Parks Rd., Oxford OX1 3AN, United Kingdom.
5. University of Bern, Institute of Geology & Oeschger Centre for Climate Change Research, Baltzerstr. 1+3 CH-3012 Bern, Switzerland.
6. Centre Scientifique de Monaco 8 Quai Antoine 1er, MC98000, Monaco.

Abstract

Rare Earth Element (REE) distributions in the ocean bear the fingerprints of several key environmental processes, including vertical particle/organic carbon fluxes, water column/pore-water oxygenation and ocean transports. The use of 'fossil' REE analyses in the service of palaeoceanography as redox, water transport or nutrient cycling 'proxies' has long been a tantalizing possibility. Here we demonstrate the application of a novel laser-ablation microanalysis approach for the rapid and accurate measurement of the REE composition of early diagenetic 'coatings' on fossil foraminifera. By applying this new method to a range of core-top and multi-core samples, we show that 'authigenic' REE enrichments on planktonic foraminifer surfaces (REEfs) reflect a primary seawater signature that becomes overprinted during sediment burial due to early diagenetic processes that control the flux of REEs to pore-fluids. Thus 'light' REEs (LREEs), and eventually 'middle' REEs (MREEs) are generally enriched in foraminifer 'coatings' relative to seawater, while Ce-anomalies (Ce/Ce*) recorded in surface sediments are typically more positive than local seawater values and are further 'eroded' during burial with the onset of anoxic conditions in the sediment. Similar

patterns have previously been observed in pore-fluid measurements. Indeed, we show that Mn and Fe concentrations measured in foraminifer 'coatings' track the availability of these elements in pore-water, indicating that they are not associated with a secondary oxide phase. We propose that these elements, along with REEs are instead adsorbed directly from pore-fluids. In contrast, U in authigenic coatings tracks the removal of this element from solution under sub-oxic conditions, supporting the use of U/Ca in foraminifer coatings as a redox proxy. Although our results confirm a significant early diagenetic influence on REEfs, we also demonstrate the potential utility of 'Ce-enrichment' relative to expected seawater values as a palaeo-oxygenation proxy. We support this proposal with down-core measurements of U/Ca and Ce-enrichment spanning the last deglaciation in the sub-Antarctic Atlantic, as well as a global array of LGM measurements, which are found to co-vary with parallel estimates of radiocarbon ventilation age, consistent with a widespread increase in the efficiency of the biological pump. Our results suggest that laser-ablation REEfs measurements may hold some promise for palaeoceanographic reconstruction, in particular through a shift in emphasis away from the reconstruction of primary seawater signals to the analysis of diagenetic impacts that are sensitive to changing hydrographic conditions.

1.0 Introduction

The Rare Earth Elements (REEs), defined here as La and the lanthanide group of elements (atomic mass 139 to 175), are particularly useful for sedimentary sourcing and environmental process 'fingerprinting' due to their highly coherent, yet non-identical, behaviour. Thus, in the marine environment, dissolved REEs are predominantly stabilised as carbonate-ion complexes, with a tendency for increased stabilisation for the heavier REEs (Byrne and Kim, 1990; Byrne and Li, 1995; Cantrell and Byrne, 1987). The partitioning of REEs between different marine phases may therefore result in fractionation between heavy- and light REEs (hereafter HREEs and LREEs respectively, defined more specifically below) (Sholkovitz et al., 1994). In addition, while the REEs are generally trivalent, Ce and Eu may also exist as Ce(IV) and Eu(II) depending on redox conditions (Byrne and Sholkovitz, 1996). Due to the lower solubility of Ce(IV), and the availability of dissolved oxygen throughout most of the open ocean, this anomalous behaviour amongst the REEs results in a characteristic depletion of Ce in seawater, which is paralleled by a converse characteristic Ce-enrichment in suspended marine particulate phases (Alibo and Nozaki, 1999; Sholkovitz et al., 1994). Since the pioneering work of (Elderfield and Greaves, 1982), and many other important studies since, the cycling of REEs within the marine environment has come to be understood as primarily involving: 1) the input of weathered REEs via riverine and atmospheric (dust)

74 fluxes; 2) fractionation of REEs via redox processes in the water column, in particular in
75 association with the removal of Ce as insoluble Ce(IV) under oxic conditions; 3) the export of
76 REEs from the surface ocean into the ocean interior and marine sediments via 'reversible
77 scavenging' (Oka et al., 2009) and particle remineralization at depth, with lower mass REEs
78 being more readily scavenged, but with Ce being relatively immune to remineralization under
79 oxic conditions (Sholkovitz et al., 1994); and 4) the transport and mixing of dissolved REEs
80 throughout the ocean basins via the ocean's large scale overturning circulation (Elderfield
81 and Greaves, 1982; Hathorne et al., 2015). Hydrothermal inputs and an additional seafloor
82 sedimentary source of REEs to seawater also make an important contribution to the total
83 marine REE budget (Abbott et al., 2015; Elderfield and Greaves, 1982). These different
84 controls on REE cycling in the marine environment are illustrated in **Figure 1**.

85 Due to the dominant controls on their cycling and fractionation, REE distributions in the
86 ocean bear the fingerprints of several key environmental and biogeochemical processes,
87 including for example the impacts of vertical particle/organic carbon fluxes, water
88 column/pore-water oxygenation and ocean transports. This raises the possibility of using
89 'fossil' REE analyses in the service of palaeoceanography, for example as redox, water
90 transport or nutrient cycling 'proxies'. However, the use of REE abundance and fractionation
91 to derive palaeoceanographic proxy information has so far been limited by two key
92 challenges: 1) the methodological challenge of efficiently and accurately measuring
93 seawater/pore-water derived REEs in sedimentary substrates; and 2) the interpretative
94 challenge of deciphering 'fossil' REE signatures preserved in deeply buried sediments in
95 terms of initial pore-water or seawater properties.

96 Some progress in addressing the first of these challenges (i.e. phase-selective analysis)
97 has previously been made through two developments: the use of 'continuous flow-through'
98 analysis to access the REE composition of what has been interpreted as primary
99 foraminiferal carbonate (Haley et al., 2005); and the use of large samples of weakly
100 chemically cleaned planktonic foraminifera to access the REE composition of what has
101 generally been interpreted as early diagenetic 'coatings' deposited from bottom-water/pore-
102 water on the outer surface of foraminifer shells (Palmer and Elderfield, 1985; Roberts et al.,
103 2012; Roberts et al., 2010). Despite their clear utility, both of these approaches still present
104 significant analytical challenges, for example due to the large sample sizes required, or the
105 difficult chemical purification and analysis procedures involved.

106 The second of the 'REE proxy challenges' identified above essentially bears on our
107 understanding of REE cycling in pore-waters, extending from the sediment-water interface
108 deep into the sediment column. Despite a wealth of research into seawater REE chemistry,
109 and on the use of Nd isotopes in particular, progress in addressing this second challenge has

arguably been more limited. One contributing factor is the relative paucity of comprehensive surveys of early diagenetic REE cycling just below the sediment-seawater interface, with a direct focus on the evolution and preservation of REE signatures in sedimentary phases. A key foundation for thinking about the 'fossil' REE preservation problem was provided by the work of (Haley et al., 2004), who proposed a model for REE cycling in pore-waters near the sediment-water interface. This conceptual model is illustrated in **Figure 1**; its principal aspects involve: 1) the transfer of REEs to the pore-water environment from seawater but principally via particulate phases that have scavenged REEs from the water column (hence typically with a LREE-enriched yet Ce-depleted signature); 2) the further release of REEs (mainly HREEs) to the pore-water environment from oxidized organic matter; 3) the subsequent release of Ce to pore-waters (typically along with Mn) under sub-oxic/anoxic conditions via the reduction of Ce(IV) and Mn-oxide phases; and 4) the reduction of Fe-oxides and mobilization of REEs with a predominantly 'middle' Rare Earth Element (MREE) enriched signature. This model would predict an offset towards lower HREE/LREE ratios and a relative enrichment in MREEs in pore-waters, relative to seawater, as is indeed suggested by sediment leachate and foraminifer 'coating' data (Du et al., 2016; Osborne et al., 2017). Furthermore, given the significant amount of REE cycling that takes place just below the sediment-water interface and the very large concentration gradient between pore-waters and seawater that this produces, it has also become apparent that the shallow sedimentary environment might exert a hitherto under-appreciated influence on seawater REE budgets and characteristics, e.g. via benthic fluxes to bottom water (Abbott et al., 2015; Du et al., 2016).

Here we demonstrate the application of a novel laser-ablation (LA-) ICPMS approach for the rapid and accurate measurement of REEs and other trace elements in early diagenetic foraminifer 'coatings' (hereafter referred to as 'foraminifer surface REE enrichments', or REEfs to convey the notion that these surface enrichments do not necessarily reflect secondary phase deposits). This approach has the particular advantages of being simple, highly efficient, and widely applicable using small aliquots of quasi-ubiquitous sample material (e.g. ~20-30 planktonic foraminifera). We show that REEfs are concentrated on the interior of planktonic foraminifer shells, and that their composition directly captures the evolving composition of pore-waters, in particular under the influence of anoxic diagenesis. While the pervasive diagenetic overprinting of REEfs is likely to preclude the recovery of primary seawater signatures, we suggest that the degree of overprinting may in some cases prove useful as a palaeoceanographic indicator.

2.0 Material and Methods

In order to limit complications from e.g. variable shell morphology or other unknown factors, monospecific samples of planktonic foraminifera (*Globigerina bulloides*, *Globigerina ruber*, *Neogloboquadrina dutertrei*, or *Globigerinoides sacculifer*; ~20-30 individuals per sample) were selected, typically from the 250-300μm size fraction, from an array of sedimentary core-top samples, as well as a short (~30cm) 'multi-core' from the Iberian Margin (SHAK-6-5M, 37.6°N, 10.1°W, 2,545m). This multi-core is known to span the latest Holocene (<5000 years) based on the stratigraphy of longer sediment cores from the same location (Hodell et al., 2015). Samples were also picked from sediment core MD07-3076 (44.1°S, 14.2°W; 3770 m water depth), spanning the last deglaciation (age model described by (Skinner et al., 2014)), as well as an array of Last Glacial Maximum (LGM) sediments. The latter LGM samples were identified on the basis of previous radiocarbon work (Skinner et al., 2017). We also present foraminiferal (authigenic) U/Ca data from core MD07-3076, obtained via solution-based analyses, as described by (Gottschalk et al., 2016). **Figure 2** shows the locations of the sediment samples used for this study.

For REE analysis, foraminifer shell chambers were individually broken open using a scalpel under the microscope, transferred to microcentrifuge tubes and ultrasonicated in methanol for ~30s to remove clays and detrital material, with repeated rinses performed until visible discoloration was absent. Up to 30 cleaned shell fragments were selected per sample and mounted on carbon tape for LA-ICPMS analysis. Note that 20-30 foraminifera equates to as little as ~200μg of carbonate, as compared to 3-25mg of carbonate required by alternative methods (Osborne et al., 2017) with comparable precision (e.g. ~2-5% RSE for elemental ratios). REE/Ca ratios of calcite were measured using a Laser Ablation- inductively coupled plasma mass spectrometry (LA-ICPMS) system in the Department of Earth Science, at the University of Cambridge. This LA-ICPMS system employs an Analyte G2 (193nm) excimer laser (Teledyne Photon Machines Inc.) coupled to a Thermo i-CapQ ICPMS to measure trace metal elemental profiles in carbonates. The system uses a large format HelEx II ablation cell, in which He gas flows to the cell and the collection cup were optimized for signal stability and washout times, and where 7 mL/min N_2 gas was added to the cell to enhance sensitivity in dry plasma mode.

The isotopes ^{25}Mg, ^{27}Al, ^{43}Ca, ^{55}Mn, ^{56}Fe, ^{66}Zn, ^{139}La, ^{140}Ce, ^{141}Pr, ^{146}Nd, ^{147}Sm, ^{151}Eu, ^{153}Eu, ^{157}Gd, ^{159}Tb, ^{163}Dy, ^{165}Ho, ^{166}Er, ^{169}Tm, ^{172}Yb, ^{175}Lu, ^{232}Th, ^{238}U were measured along the laser profile tracks. Each laser profile was aligned along a shell surface to improve consistency of ablated material. We also pre-ablated each track before measurement to remove ~0.3 μm of the surface. Pre-ablation was done using a laser spot of 15 x 60 μm, at a frequency of 3 Hz, a tracking speed of 12 μm/s and a laser fluence of 1.2J/cm^2. This pre-ablation significantly improved signal stability and eliminated spikes in Mg, Al, Mn, Fe, which

183 are commonly associated with surface contamination by clay particles. For REE
184 measurement, the Laser Ablation system was optimised for high spatial resolution using a slit
185 aperture of 20x40 µm, a frequency of 7 Hz and a 1.2J/cm^2 laser fluence. The laser tracking
186 speed was set at 2 µm/s, resulting in the removal of the top ~2 µm of the shell surface for
187 REE measurements. Each measurement (including background collection, pre-ablation,
188 ablation and tail-off to background) thus required ~90-120s.
189
190 We used a Thermo i-CapQ ICPMS collision cell in kinetic energy discrimination (KED)
191 mode to minimize interferences on transitional mass elements (Tanner et al., 2002). Helium
192 flow in the collision cell was tuned using ^{56}Fe mass to maximize the signal to noise ratio. The
193 ICP-MS sensitivity was also optimized using NIST612 reference glass material for maximum
194 sensitivity across Mg-U mass range and maintaining ThO/Th <0.5% and Th/U ratio ~1. Data
195 reduction involved initial screening of spectra for outliers, subtraction of the mean
196 background intensities (measured with the laser turned off between every one to three
197 ablations), internal standardisation to ^{43}Ca, and external standardisation using the NIST-
198 SRM612 glass reference material. The internal standardisation to ^{43}Ca was deemed to be
199 appropriate as all of our measurements were obtained from foraminiferal calcite. This was
200 confirmed by monitoring the stability of ^{43}Ca intensities over several analytical sessions and
201 comparing these with ^{43}Ca intensities obtained by drilling through the same shell using the
202 LA-ICPMS. Both approaches (i.e. drilling through the shell and surface tracks) delivered
203 identical Ca intensities confirming that our surficial analyses primarily targeted foraminiferal
204 calcite.
205
206 Signals of Mg, Al, Mn, Fe were used to monitor clay contamination and any values
207 above 1 mmol/mol (Mn/Ca) or 0.25 mmol/mol (Al/Ca) were removed from the averaged
208 dataset. The sample average REE concentrations were calculated by averaging
209 compositions along each ablation profile (after background subtraction and normalization),
210 and then averaging all profiles from 20-30 shell fragments per sample. As discussed further
211 below, inter-shell scatter in element concentration ratios was relatively small, so that the
212 averaging procedure typically resulted in a estimated uncertainties of ~1-5% RSE (see
213 supplementary Figure S1), consistent with an external analytical precision of ~10% RSD (see
214 below).
215
216 In-house *eBlue* calcite standards and NIST-SRM614 were used to monitor long-term
217 standard reproducibility. The internal precision was 1% RSE for all analytes on average, and
218 0.81, 1.06, 0.87, 1.28, 1.43,1.04, 1.93, 0.98, 1.50, 1.03, 1.10, 1.00, 1.31, 1.02, and 0.86%
219 RSE for La, Ce, Pr, Nd, Sm, Eu, Gd, Tb, Dy, Ho, Er, Tm, Yb, Lu, U respectively. Long-term

external precision of NIST-SRM614 based on 6 analytical days was 5% RSD. This compares well with other recent studies (e.g. (Osborne et al., 2017). The internal precision of NIST-SRM612 elemental ratios was 0.6% RSD. Measured concentrations of NIST-SRM614 are within 8% of expected concentrations (Jochum et al., 2011). The internal reproducibility of our in-house carbonate standard (*eBlue*) is 12% RSE, and is larger than for our other standards primarily due to the inhomogeneity of the carbonate material.

Supernatant seawater recovered from the multi-core site SHAK-6-5M was also analysed for its REE composition. Shipboard salinity measurements performed on the supernatant seawater were used to confirm that the multi-core seal had remained intact, and that the bottom water samples had not been contaminated during recovery. REEs were determined using Fe-coprecipitation and isotope dilution (modified from the method of (Greaves et al., 1989)), followed by instrumental determination by ICP-MS (after methods detailed in (Rousseau et al., 2013; Zheng et al., 2014) and (Behrens et al., 2016)). Briefly, 40 ml of filtered, acidified seawater (pH ~2) was weighed into a pre-cleaned 50ml centrifuge tube,and a mixed REE spike added for isotope dilution analysis plus 50 µg Fe as $FeCl_3$ (Greaves et al., 1989). After mixing and allowing to stand overnight to ensure equilibration, the pH was raised to pH 7.5 +/- 0.5 by addition of ~0.1M ammonia solution. The sample was left for > 3 days to allow the $Fe(OH)_3$ precipitate to settle, then centrifuged. The precipitate was transferred to a 0.5ml microcentrifuge tube in 250 µl water where centrifugation and rinsing were repeated three times. The precipitate was dissolved in 500 µl 0.1M HCl and a 20 µl subsample taken for determination of Fe recovery by ICP-OES, together with Na, Mg, Ca, K and Ba, monitored to check their removal. REE were measured in the remaining solution by ICP-MS on a Thermo ElementXR, fitted with an ESI Apex IR desolvating system using N_2 as additional gas to reduce oxide formation and a 50 µl/min PFA microflow nebulizer. This combination enabled BaO/Ba < 0.02 %, LaO/La and CeO/Ce < 0.4 %, and PrO/Pr < 0.25 %, consistent with oxide formation levels found by (Rousseau et al., 2013) using an ESI Apex-Q. Corrections for Barium oxide, REE oxides and REE isobaric interferences were done offline. Ce, Nd, Sm, Eu, Gd, Dy, Er, Yb and Lu concentrations were calculated by isotope dilution and La, Pr, Tb, Ho and Lu calculated against an external mixed REE standard with the isotope dilution calculated REE used as internal standards to correct for the $Fe(OH)_3$ co-precipitation yield (Rousseau et al., 2013; Zheng et al., 2014). $Fe(OH)_3$ co-precipitation reduces seawater [Ba] to a level similar to that of [La] (Greaves et al., 1989) but this remains too high to allow correction of ^{138}Ba isobaric interference on ^{138}La without further chemical separation. Therefore, the La concentration was calculated using ^{139}La, analogous to the mono-isotopic REE (Behrens et al., 2016).

Pore-water samples were extracted from multi-core SHAK-6-5M onboard ship at 1 cm intervals using Rhizon samplers (Seeberg-Elverfeldt et al. 2005) and preserved for analyses of trace metals by acidification to pH ≈ 2 with HNO_3. Fe and Mn were determined by ICP-OES using an Agilent 5100 instrument, after dilution to a constant Na concentration of ~ 110 ppm. U was determined by ICPMS on a Thermo ElementXR mass spectrometer, after further dilution to 10 ppm Na in order to minimize Na input to the mass spectrometer, adapting the method of (Misra et al., 2014) for the determination of multiple element/Ca ratios in foraminifera. In situ micro-sensor oxygen measurements performed onboard ship at the time of recovery of SHAK-6-5M were calibrated using oxygen solubility at the measured salinities (37PSU) and temperature according to the Unisense Gas tables (Garcia and Gordon, 1992). A two-point linear calibration was applied with oxygen values from the overlying water (assuming air saturation upon bubbling with air) and in the anoxic part of the sediment.

3.0 Results

3.1 Interior versus exterior REE enrichment on foraminifer shell surfaces

Our LA-ICPMS analyses demonstrate that REEs are concentrated on the *interior* surface of planktonic foraminifer shells, rather than on the exterior surface. It is possible that this very thin surface enrichment hay have been missed in previous studies (Tachikawa et al., 2013). As shown in **Figure 3**, while the interior surfaces of the foraminifer shells are characterized by far higher REE concentrations, and while there is a significant degree of variability in absolute REE concentrations between individual foraminifer shells in a given core-top sediment sample (**Figure 3a**), both the internal and external surfaces of foraminifer shells record a similar 'REE composition' (i.e. the same enrichment of the REE relative to each other) (**Figure 3b**). We thus observe relatively constant REE composition (despite variable total concentrations) between individual foraminifer fragments within a given population (i.e. sample). The precision of our REEfs determinations, taking into account the scatter within a population of foraminifer fragments, therefore scales with the base analytical uncertainty (e.g. ~10% RSD, for SRM-NIST614) divided by the square root of the total number of fragments analysed (see supplementary Figure S1). A precision of ~2-5% RSE can thus be obtained for 20-30 fragments analysed per sample. Based on these results, we hereafter we report REEfs based on measurements of the interior surfaces of ~20-30 foraminifer shells, which present higher concentrations than the exteriors and provide for slightly better analytical precision as a result.

3.2 Global core-top REEfs array: assessing seawater influence

In **Figure 4** we show that sedimentary core-top REEfs obtained via LA-ICPMS analysis indeed reflect a seawater origin, yielding a typical 'seawater signature' that is characterized by a relative depletion of light REEs (LREEs, defined as [Pr+Nd]/2; (Haley et al., 2004)) as compared to heavy REEs (HREEs, defined as [Yb+Lu]/2; (Haley et al., 2004)), and a distinct depletion in Ce (i.e. 'Ce-anomaly', here denoted by Ce/Ce* and defined as 2*Ce/[La+Pr]; (de Baar et al., 1985)), where all REE concentrations are normalized to the composition of Post-Archaean Australian Shale (PAAS) (Pourmand et al., 2012). This typical seawater signature rules out a predominantly clay- or terrigenous clastic contamination origin for REEfs. The typical LREE/HREE depletion observed in deep ocean seawater arises from the enhanced stabilization of HREEs in solution via complexation and the greater capacity for LREE removal from the water column via particle absorption (Sholkovitz et al., 1994). Seawater Ce-anomalies (Ce/Ce*) develop as a result of the exclusive loss of Ce from the water column through the generation of insoluble Ce(IV) oxides under oxic conditions (de Baar et al., 1985; Elderfield and Greaves, 1982; German et al., 1995; Sholkovitz et al., 1994) in parallel with the progressive enrichment of other REEs via vertical particle fluxes (Alibo and Nozaki, 1999). In capturing this typical seawater signature, our LA-ICPMS REEfs analyses are consistent with measurements performed on dissolved 'weakly cleaned' (i.e. cleaned for detrital contamination only) planktonic foraminifer shells from sedimentary core-tops (Osborne et al., 2017; Wilson et al., 2013). The latter also consistently exhibit a depletion in HREE as compared to seawater, which our comparison of seawater REE and LA-ICPMS REEfs from either side of the sediment-water interface confirms (**Figure 4**).

3.3 Global trends in core-top foraminifer surface- and seawater REE composition compared

Figure 5 shows a comparison of global trends in middle rare earth enrichment (MREE/MREE*, defined as (2[Tb+Dy]/[Pr+Nd+Yb+Lu], PAAS-normalised; (Haley et al., 2004)) *versus* HREE/LREE enrichment, as exhibited in both core-top REEfs and seawater data (seawater data is shown only for sites near our core-top locations, for direct comparability). As previously observed in core-top bulk sediment leachate REE data (Du et al., 2016) and dissolved 'weakly cleaned' foraminifer REE data (Osborne et al., 2017), our core-top REEfs data exhibit a general tendency for lower MREE/MREE* and higher HREE/LREE when moving from the North Atlantic, via the Southern Ocean and Indian basins, to the Pacific basin. This pattern mimics a broadly similar trend observed in global seawater data (Osborne et al., 2017), albeit with a general offset towards lower HREE/LREE and higher MREE/MREE* measured in sedimentary substrates (i.e. authigenic phases). This pattern (and offset from seawater data), has previously been described in terms of a global 'authigenic/pore-water array' (Du et al., 2016). The observed global trend in seawater REE compositions, which is essentially expressed along the dominant deep-water flow trajectory

from the North Atlantic to the Pacific, has been interpreted to reflect a combination of inherently greater fluvial/aeolian delivery of lithogenic material with an elevated MREE signature to the Atlantic as compared to the Southern Ocean and Pacific (Osborne et al., 2017), as well as the progressive nutrient-like enrichment of HREE/LREE in deep water due to preferential scavenging of LREEs from the water column (e.g. Alibo and Nozaki, 1999; Hathorne et al., 2015; Sholkovitz et al., 1994). On these premises, conservative mixing between water masses would be responsible for the smooth inter-basin trends observed in the seawater data (Hathorne et al., 2015).

The widespread depletion of 'authigenic-phase' HREE/LREE, as compared to seawater, has been interpreted by (Osborne et al., 2017) to reflect the preferential adsorption of LREEs onto foraminifer surfaces (Byrne and Kim, 1990; Cantrell and Byrne, 1987), thus lowering the HREE/LREE of foraminifer surfaces, presumably while also increasing the HREE/LREE of seawater (or pore water). However, this interpretation is not easily reconciled with the fact that pore-waters (like foraminifera) exhibit an offset to higher MREE/MREE* and lower HREE/LREE as compared to seawater (Haley et al., 2004). Below we discuss an alternative proposition that the offset between seawater- and authigenic-phase REE compositions directly mirrors an offset between seawater- and pore-water REE compositions.

3.4 Sedimentary REEfs analyses below the sediment-seawater interface

REEfs measurements performed on a 30cm multi-core recovered from the Iberian Margin (see Methods) are shown in **Figure 6**, and demonstrate how the concentrations of all REEs – with the exception of Ce – rapidly increase across the first few centimeters beneath the sediment-water interface. As shown in **Figure 7**, MREE/MREE* and HREE/LREE recorded in the same foraminifer 'coatings' increase and decrease respectively within the first 2cm, more rapidly than the total concentration of REEs (note the reversed scale for HREE/LREE in **Figure 7**). Notably, Ce concentrations in the foraminifer 'coatings' only increase significantly once pore-water oxygen levels reach sub-oxic levels, reflecting the release of Ce to pore-waters via the reduction of Ce-oxides (presumably that have been stripped from the overlying water column). The presence of Ce in the 'coatings' thus tracks the concentrations of Mn and Fe in both the 'coatings' and the pore-waters (**Figure 7**), in the sense that they all show a significant increase below the zero oxygen level. In contrast, U in the foraminifer 'coatings' records opposing changes as compared to pore-water [U] (note reversed scale for pore-water [U] in **Figure 7**).

4.0 Discussion

4.1 Assessing pore-water influence on REEfs

As shown in **Figure 7**, Mn and Fe in the foraminifer 'coatings' track the availability of these elements as dissolved ions in the pore-waters, demonstrating that these elements are not associated with an authigenic oxide phase deposited on the foraminifer surfaces. Rather, it would appear that they are directly adsorbed onto the foraminifer surface or partitioned into secondary or recrystalizing/altered foraminifer calcite phases. We speculate that REEs are transferred to the foraminifer 'coatings' in a similar manner, such that REEfs provide a direct record of pore-water REE chemistry as it evolves beneath the sediment-water interface. This inference is supported by the observed link between Ce/Ce* and Mn in the foraminifer 'coatings' (**Figure 7**), which are also expected to be coupled in pore-waters (Haley et al., 2004). On the other hand, U/Ca would appear to provide a record of U-flux to the sediments from the overlying seawater, supporting the proposal that U/Ca might provide a proxy for bottom-water oxygenation (Boiteau et al., 2012), e.g. via its influence on pore-water/seawater oxygenation gradients and therefore the flux of U to sediments (Klinkhammer and Palmer, 1991). The apparently different incorporation mechanisms for U *versus* Mn (at least in this context), suggests that some caution might be warranted in the use of authigenic U/Mn ratios as a redox proxy, in preference to U/Ca ratios for example (Gottschalk et al., 2016).

Although parallel pore-water REE measurements would be needed to fully test the above inferences, it is notable that the multi-core REEfs shown in **Figure 7** exhibit essentially the same behavior as observed in pore-waters from the Pacific (Haley et al., 2004), with rapid REE concentration increase below the sediment-water interface and subsequent Cerium increase under sub-oxic conditions, as well as relative LREE enrichment and the development of a MREE 'bulge'. In order to illustrate this similarity, **Figure 8** shows a comparison of the REEfs data from SHAK-6-5M with the pore-water data of (Haley et al., 2004), both set within the context of the global 'authigenic/pore-water array' (Du et al., 2016). The data in **Figure 8** show that, when moving from seawater just above the sediment-water interface (square symbols in **Figure 8**) down into the sediment column, pore-water REE compositions evolve along the global array, rapidly shifting from a seawater regime (open circles in **Figure 8**), via the highly oxic bottom-water/pore-water regime (filled squares in Figure 8) to the sub-oxic pore-water/authigenic regime (open stars in **Figure 8**). The multi-core data from SHAK-6-5M suggest that REE-enrichments on foraminifer shells follow the same general trajectory.

4.2 The proxy potential of deeply buried REEfs signatures: cause for optimism?

Seawater REE distributions are influenced by the large-scale circulation- and mixing of the ocean, primarily through its interaction with vertical particle fluxes (Oka et al., 2009). In

particular, it has been proposed that: 1) the progressive increase in HREE/LREE, or for example Er/Nd (Bertram and Elderfield, 1993), along a dominant water flow trajectory from the North Atlantic to the North Pacific arises from the greater stabilization of HREEs in solution via complexation and the preferential scavenging of LREEs from the water column during water transport; and 2) the progressive depletion of Ce relative to other LREEs, producing a so-called Ce-anomaly (Ce/Ce*), develops in proportion to the amount of time that water has spent being transported under oxic conditions favoring insoluble Ce(IV) oxide formation and loss from the water column, as well as the regeneration of neighboring LREEs (Alibo and Nozaki, 1999; German et al., 1995). Both of these characteristics of marine REE distributions would in principle lend themselves to the development of 'proxies' for water provenance, particle flux and/or 'ventilation' (in a sense broadly similar to that often used in reference to stable carbon isotopes, which reflect an interaction between regionally determined 'preformed' values, mixing, and regeneration at depth and along flow paths) (Hathorne et al., 2015; Zheng et al., 2016).

Our observation that REE-enrichments are present on both the interior and exterior surfaces of the foraminifer shells but are significantly more concentrated on the interior surfaces strongly argues for a micro-environment influence on the transfer of REEs to the foraminifer shells, but a macro-environment (i.e. pore-water chemistry) control on the availability of these elements for incorporation. We speculate that the transfer of REEs to foraminifer shells is aided by the partial dissolution and/or recrystallization of the shells, which might be enhanced on their interior due to organic carbon respiration, as well as the enhanced REE concentrations that occur in pore-waters. The latter occurs as a result of REE fluxes to the pore-waters from sedimentary and other sources, perhaps in association with a drop in pore-water pH and therefore the carbonate ion complexation of REEs in solution. These considerations raise the question: to what extent are REEfs indicative of seawater *versus* pore-water composition, and to what extent may these differ, both at the sediment-water interface, and with deeper burial?

The results from multi-core SHAK-6-5M (**Figure 6**) indicate that REEfs and other elements associated with them bear a strong pore-water influence, which evolves over the upper sediment pile in response to redox changes in particular. This interpretation is further supported by the trends shown in **Figure 7** and **Figure 8**, which are consistent with the pore-water model of (Haley et al., 2004), where the transition from seawater to oxic pore-water, to anoxic pore-water principally involves the staged enrichment of LREEs, Ce and MREEs due to the release of scavenged elements from hemipelagic particulate phases and the eventual reduction of Ce(IV) and Fe-oxides (Haley et al., 2004). Our results suggest that this process

affects the REE composition of both pore-waters and foraminifer 'coatings'. The most important REE sources and sinks in this environment, and their controls, might eventually be elucidated using explicit models of REE cycling in the marine sedimentary environment. Indeed, given the strong connections between the sedimentary, pore-water and seawater regimes, it seems reasonable to conclude that models of seawater REE cycling are unlikely to be adequately complete in the absence of a sedimentary/pore-water component that permits REE fluxes across the sediment-water interface (Abbott et al., 2015; Elderfield and Greaves, 1982). This also raises questions regarding the long-term evolution of REE signatures (and likely also REE isotopes) in authigenic phases and their link to seawater chemistry and/or sediment composition. In particular, if REEfs include a significant early diagenetic pore-water influence, to what extent is it possible to use these measurements to reconstruct the evolution of past seawater composition?

Our results are consistent with previous work on pore-waters, sediment leachates and foraminifer-associated REEs (Du et al., 2016; Haley et al., 2004; Haley et al., 2005; Osborne et al., 2017) in showing that down-core HREE/LREE and Ce/Ce* are unlikely to capture an evolving seawater signal, as both of these metrics are substantially altered near the sediment-water interface (e.g. **Figure 7** and **Figure 8**). A further comparison of core-top REEfs with seawater data selected from nearest available locations confirms that seawater Ce-anomalies are generally not preserved in foraminifer 'coatings', although it is important to stress that this comparison necessarily involves some extrapolation between seawater and core-top locations. **Figure 9a** also shows that core-top Ce/Ce* values are generally higher than their seawater counterparts, resulting in $Ce^*_{core\text{-}top}/Ce^*_{seawater}$ values generally >1, especially under lower oxygen conditions. Hereafter we refer to the $Ce^*_{core\text{-}top}/Ce^*_{seawater}$ ratio as a measure of 'Ce-enrichment'. Notably, the data of (Haley et al., 2005) from both benthic and planktonic foraminifera (analysed by 'flow-through dissolution') also appear to fit the general pattern of greater Ce-enrichment under lower oxygen conditions, suggesting that these data might also reflect a predominantly pore-water signature.

A link between Ce-enrichment and deep water oxygenation might indeed be expected, given that the supply of oxygen to pore-waters should influence the capacity for Ce(IV) reduction, and therefore the release of 'excess Ce' for adsorption onto foraminifera just below the sediment-water interface. The degree of scatter in **Figure 9a** is perhaps not surprising either, as it is entirely possible that the full amount of Ce-enrichment achievable at a given location (e.g. as determined by prevailing bottom water oxygenation, but also sedimentation rates and organic carbon fluxes) may not always be realized immediately below the sediment-water interface (here typically within the top 3cm). **Figure 9b** supports this interpretation, showing a tighter correlation between *in situ* bottom water oxygenation

478 measurements and the degree of Ce-enrichment recorded in foraminifer 'coatings' that are
479 sub-modern, but have already passed through the oxic to sub-oxic transition (typically ~16cm
480 below the sediment-water interface in this context). Foraminifer coating U/Ca ratios
481 measured in parallel are also found to scale closely with Ce-enrichment and bottom water
482 oxygenation, supporting the use of U/Ca ratios as a proxy for deep-water oxygenation
483 (Boiteau et al., 2012; Gottschalk et al., 2016). Notably, **Figure 9b** shows directly coupled *in*
484 *situ* foraminifer and bottom-water measurements, rather than the interpolated values adopted
485 for **Figure 9a**, which might also contribute to the tighter relationships that are observed.
486 These results provide tentative support for the use of Ce-enrichment in down-core sediments
487 (i.e. the degree of Ce/Ce* increase relative to a modern reference modern well below the
488 oxic-sub-oxic/anoxic transition) as a bottom-water oxygenation proxy. This would represent a
489 slight modification of previous proposals to use Ce/Ce* directly as a bottom-water
490 oxygenation proxy, which has previously been shown to be problematic (German and
491 Elderfield, 1990). Clearly, the Ce-enrichment proxy (as we have defined it) would optimally
492 apply to locations where past seawater Ce/Ce* changes have been small compared to pore-
493 water changes, and we further speculate that it would work best where seawater has
494 remained oxic, and where pore-waters/sediments pass relatively quickly through the oxic to
495 sub-oxic transition.
496
497 Further work is clearly needed to fully assess the proxy-potential of 'Ce-enrichment'
498 and other REEfs metrics, using a wider range of carefully selected core-top material, where
499 the influences of local bottom water oxygenation, organic carbon fluxes, sediment
500 composition and sedimentation rates (hence REEfs 'lock-in depth') have all been assessed.
501 Nevertheless, initial down-core results suggest that some optimism might be warranted. Thus
502 as shown in **Figure 10**, and similar to observed in our core-top data, down-core
503 measurements of Ce-enrichment and U/Ca-enrichment in core MD07-3076 from the deep
504 sub-Antarctic Atlantic (Skinner et al., 2010; Skinner et al., 2013) are both found to decrease
505 with radiocarbon ventilation ages across the last deglaciation. The transition in Ce-
506 enrichment across the deglaciation is notably more gradual than observed in radiocarbon
507 and U/Ca, as has also been observed for Nd isotopes measured in this core (Skinner et al.,
508 2013). Whether or not this implies the influence of additional controls on Ce-enrichment,
509 including changing seawater properties (or indeed vertical particle fluxes), is difficult to
510 evaluate at this stage. However, the apparent increase in the influence of North Atlantic
511 sourced deep-water across the last deglaciation that is suggested by the Nd isotope data
512 (Skinner et al., 2013) would not be able to explain the decrease in Ce-enrichment that is
513 observed in parallel, as North Atlantic deep-water is currently more enriched in Ce than its
514 southern and/or Pacific counterparts (Alibo and Nozaki, 1999; German et al., 1995).

Futhermore, it can be shown that the Ce-enrichment and U/Ca data in **Figure 10** are approximately logarithmically scaled, suggesting that Ce-enrichment might saturate quickly (due to the fact that the supply of Ce to pore-fluids from dispersed oxides may be limited), while U/Ca does not saturate at all (due to the fact that there is practically an unlimited supply of U from seawater that can continually increase as the U concentration gradient between bottom water and pore-waters increases, and the zero oxygen level approaches the sediment-water interface).

Figure 10 also shows how LA-ICPMS U/Ca ratios track paired solution-ICPMS U/Ca ratios measured in the same sediment core (Gottschalk et al., 2016). The LA-ICPMS results yield higher absolute values, as would be expected given that these measurements directly target the authigenic surface enrichments, whereas the solution-ICPMS results are based on the analysis of the whole foraminifer shells and therefore provide a 'diluted' authigenic coating signal (Gottschalk et al., 2016). It is also notable that core-top Ce/Ce* values in this sediment core are enriched relative to expected seawater values only by a factor of ~1.3 (German et al., 1995), and down-core Ce/Ce* values remain <1 except in LGM sediments, suggesting that Ce/Ce* is sensitive to even relatively subtle early diagenetic overprinting of REE signatures.

Further support for the potential use of Ce-enrichment and U/Ca measured in foraminifer 'coatings' as potential palaeo-redox proxies comes from LA-ICPMS measurements performed on a global array of marine sediments from the Last Glacial Maximum (LGM, ~18-23 ka BP), shown in **Figure 11**. These again demonstrate a tendency for greater Ce-enrichment and greater U/Ca-enrichment in planktonic foraminifer 'coatings' in parallel with larger increases in local deep-water radiocarbon ventilation ages (Skinner et al., 2017). If these initial results can be confirmed, they would be significant in confirming a widespread lowering of deep-water oxygen concentrations (Jaccard and Galbraith, 2012), in parallel with reduced radiocarbon ventilation (Skinner et al., 2017). This in turn would support the inference of a larger respired carbon inventory in the LGM ocean, driven specifically by reduced ocean ventilation contributing to a more efficient biological pump (e.g. Skinner et al., 2017). Quantification of the implied respired carbon inventory change via 'absolute' oxygenation estimates (e.g. McCorkle and Emerson, 1988) would permit a more accurate assessment of the eventual impact on atmospheric CO_2. While our results suggest that LA-ICPMS analyses on early diagenetic foraminifer 'coatings' hold some promise for palaeoceanographic reconstruction, and for palaeo-redox reconstruction in particular, an attempt at quantitative inferences must await a full core-top calibration study, where the processes operating near the sediment-water interface and deeper in the sediment column

552 can be more fully assessed across the full range of sedimentary and hydrographic
553 conditions.
554
555 **5.0 Conclusions**
556 We have demonstrated the application of a novel and powerful LA-ICPMS method for
557 the analysis of early diagenetic 'coatings' of foraminifera, including their Rare Earth Element
558 composition (REEfs). By virtue of its relative simplicity and rapidity, this method opens the
559 door to a wide range of studies targeting the behavior of REEs in the marine sedimentary
560 environment. This method has allowed us to show that REEs are more highly enriched on
561 the interior surfaces of planktonic foraminifer tests than their exterior surfaces, although
562 similar REE signatures are found on both. This provides a clue as to the origin of REEfs
563 enrichments, which we show have a significant early diagenetic component. Indeed, we
564 show that although REEfs bear a distinctive 'marine REE signature', with a characteristic
565 LREE versus HREE depletion and Ce-anomaly (Ce/Ce*), they also exhibit the effects of early
566 diagenetic overprinting near the sediment-water interface. The most obvious early diagenetic
567 impact on REEfs compositions is an offset toward lower HREE/LREE and higher
568 MREE/MREE* values, as compared to expected seawater values (notably this implies the
569 addition of Nd for example). During burial, REEfs evolve along a global 'authigenic/pore-
570 water array', away from the oxic seawater regime, via an oxic pore-water regime, to a sub-
571 oxic pore-water/authigenic regime, as observed in pore-waters. REEfs are thus shown to
572 directly track the evolving composition of pore-waters; a conclusion that is supported by the
573 fact that Fe and Mn measurements made in parallel by LA-ICPMS track the availability of
574 these elements in pore-waters, rather than as a insoluble oxide phase for example. These
575 results raise questions regarding the utility of REEfs concentration/isotope measurements
576 (whether obtained by LA-ICPMS, or by standard analysis of 'unclean foraminifera' or
577 sediment leachates) for palaeoceanographic proxy reconstructions. Notably, potential
578 hydrographic REE indicators such as HREE/LREE ratios or Ce/Ce* are clearly overprinted in
579 marine sediments via early diagenesis. However, we show that the degree of this
580 overprinting might instead serve as a viable proxy for hydrographic conditions. More
581 specifically, Ce-enrichment in core-top sediments (i.e. the supply of 'excess' Ce to pore-
582 waters, relative to that expected from local seawater Ce/Ce* values) tends to track the
583 deposition of U (producing higher U/Ca ratios in foraminifer 'coatings') under conditions of
584 lower bottom water oxygenation. This raises the potential of a viable REE-based palaeo-
585 oxygenation proxy, ideally for application in marine sediments that rapidly pass through an
586 oxic- to sub-oxic transition, and where the supply of oxygen from bottom water is the main
587 control on Ce-oxide reduction near the sediment-water interface. Down-core records from
588 the sub-Antarctic Atlantic show that Ce-enrichment tracks both U/Ca and radiocarbon

589 ventilation across the last deglaciation, consistent with previous interpretations of increasing
590 deep-water ventilation at this location in the sub-Antarctic Atlantic across the last deglaciation
591 (Skinner et al., 2010; Gottschalk, 2016). Notably, similar relationships are also observed in a
592 global array of LGM sediments, which provide evidence for an enhanced respired carbon
593 inventory in the LGM ocean, with implications for the mechanisms of atmospheric CO_2 draw-
594 down in a glacial world. These results suggest that the use of REEfs in the service of
595 palaeoceanography holds some promise, in particular via a shift in emphasis away from the
596 interpretation of 'primary' hydrographic REE signals, toward the interpretation of early
597 diagenetic effects that are sensitive to changing hydrographic conditions. However, before
598 the full potential of REEfs analyses may be accessed, more work will need to be done to
599 elucidate the full sedimentary- and hydrographic dependence of REE mobilization and
600 incorporation into foraminifer 'coatings'. Our novel LA-ICPMS approach provides an efficient
601 means of tackling this.
602
603 **Acknowledgements**
604 We are deeply indebted to Harry Elderfield, whose prior work inspired this study, and who
605 helped on board the R/V James Cook during cruise JC089 to recover sediments and extract
606 pore-waters that have been analyzed in this study. We also thank Sambuddha Misra for his
607 invaluable assistance in setting up a protocol for trace element and REE analysis in seawater
608 and pore-waters, as well as Maximillian Traynor who performed the pore-water trace-element
609 measurements. We are grateful to David Hodell, Nick McCave and all the participants of the
610 JC089 cruise on board the R/V James Cook for their assistance in recovering materials that
611 were used in this study. This work was made possible by NERC grants NE/J00653X/1 and
612 NE/L006421/1.
613
614 **References**

Abbott, A.N., Haley, B.A., McManus, J. and Reimers, C.E. (2015) The sedimentary flux of dissolved rare earth elements to the ocean. Geochimica et Cosmochimica Acta 154, 186-200.

Alibo, D.S. and Nozaki, Y. (1999) Rare earth elements in seawater: particle association, shale normalization, and Ce oxidation. Geochimica et Cosmochimica Acta 63, 363-372.

Behrens, M.K., Muratli, J., Pradoux, C., Wu, Y., Böning, P., Brumsack, H.-J., Goldstein, S.L., Haley, B., Jeandel, C., Paffrath, R., Pena, L.D., Schnetger, B. and Pahnke, K. (2016) Rapid and precise analysis of rare earth elements in small volumes of seawater – method and intercomparison. Marine Chemistry 186, 110-120.

Bertram, C.J. and Elderfield, H. (1993) The geochemical balance of the rare earth elements and neodymium isotopes in the oceans. Geochimica et Cosmochimica Acta 57, 1957-1986.

Boiteau, R., Greaves, M. and Elderfield, H. (2012) Authigenic uranium in foraminiferal coatings: A proxy for ocean redox chemistry. Paleoceanography 27.

Byrne, R.H. and Kim, K.-H. (1990) Rare earth element scavenging in seawater. Geochimica et Cosmochimica Acta 54, 2645-2656.

Byrne, R.H. and Li, B. (1995) Comparative complexation behaviour of the rare earths. Geochimica et Cosmochimica Acta 59, 4575-4589.

Byrne, R.H. and Sholkovitz, E.R. (1996) Chapter 158 Marine chemistry and geochemistry of the lanthanides, Handbook on the Physics and Chemistry of Rare Earths. Elsevier, pp. 497-593.

Cantrell, K.J. and Byrne, R.H. (1987) Rare earth element complexation by carbonate and oxalate ions. Geochimica et Cosmochimica Acta 51, 597-605.

de Baar, H.J.W., Bacon, M.P. and Brewer, P.G. (1985) Rare earth elements in the Pacific and Atlantic Oceans. Geochimica et Cosmochimica Acta 49, 1943-1959.

Du, J., Haley, B.A. and Mix, A.C. (2016) Neodymium isotopes in authigenic phases, bottom waters and detrital sediments in the Gulf of Alaska and their implications for paleo-circulation reconstruction. Geochimica et Cosmochimica Acta 193, 14-35.

Elderfield, H. and Greaves, M.J. (1982) The rare earth elements in seawater. Nature 296, 214-219.

Garcia, H.E. and Gordon, L.I. (1992) Oxygen solubility in seawater- better fitting equations. Limnology and Oceanography 37, 1307-1312.

Garcia, H.E., Locarnini, R.A., Boyer, T.P., Antonov, J.I., Baranova, O.K., Zweng, M.M., Reagan, J.R. and Johnson, D.R. (2014) World Ocean Atlas 2013, Volume 3: Dissolved Oxygen, Apparent Oxygen Utilization, and Oxygen Saturation, in: Levitus, S., Mishonov, A.V. (Eds.), NOAA Atlas NESDIS 75. U.S Government Printing Office, Washington D.C., p. 27.

German, C.R. and Elderfield, H. (1990) Application of the Ce anomaly as a paleoredox indicator: the ground rules. Paleoceanography 5, 823-833.

German, C.R., Masazuwa, T., Greaves, M., Elderfield, H. and Edmond, J.M. (1995) Dissolved rare earth elements in the Southern Ocean: Ce oxidation and the influence of hydrography. Geochimica et Cosmochimica Acta 59, 1551-1558.

Gottschalk, J., Skinner, L.C., Lippold, J., Vogel, H., Frank, N., Jaccard, S.L. and Waelbroeck, C. (2016) Biological and physical controls in the Southern Ocean on past millennial-scale atmospheric CO2 changes. Nature Communications 7, 11539.

Greaves, M. (1988) The Determination of the Rare Earth Elements in Seawater and their Distribution in the N.E. Atlantic Ocean. University of Leeds, Leeds, p. 135 pp.

Greaves, M.J., Elderfield, H. and Klinkhammer, G.P. (1989) Determination of the rare earth elements in natural waters by isotope-dilution mass spectrometry. Analytical Chemistry 218, 265–280.

Haley, B.A., Klinkhammer, G. and McManus, J. (2004) Rare earth elements in pore waters of marine sediments. Geochimica et Cosmochimica Acta 68, 1265-1279.

Haley, B.A., Klinkhammer, G.P. and Mix, A.C. (2005) Revisiting the rare earth elements in foraminiferal tests. Earth Planet. Sci. Lett. 239, 79-97.

Hathorne, E.C., Stichel, T., Brück, B. and Frank, M. (2015) Rare earth element distribution in the Atlantic sector of the Southern Ocean: The balance between particle scavenging and vertical supply. Marine Chemistry 177, Part 1, 157-171.

Hodell, D., Lourens, L., Crowhurst, S., Konijnendijk, T., Tjallingii, R., Jiménez-Espejo, F., Skinner, L., Tzedakis, P.C., Abrantes, F., Acton, G.D., Zarikian, C.A.A., Bahr, A., Balestra, B., Barranco, E.L., Carrara, G., Ducassou, E., Flood, R.D., José-Abel, F., Furota, S., Grimalt, J., Grunert, P., Hernández-Molina, J., Kim, J.K., Krissek, L.A., Kuroda, J., Li, B., Lofi, J., Margari, V., Martrat, B., Miller, M.D., Nanayama, F., Nishida, N., Richter, C., Rodrigues, T., Rodríguez-Tovar, F.J., Roque, A.C.F., Goñi, M.F.S., Sánchez, F.J.S., Singh, A.D., Sloss, C.R., Stow, D.A.V., Takashimizu, Y., Tzanova, A., Voelker, A., Xuan, C. and Williams, T. (2015) A reference time scale for Site U1385 (Shackleton Site) on the SW Iberian Margin. Global Planet. Change 133, 49-64.

Jochum, K.P., Stoll, U.W., Brigitte, Kuzmin, D., Yang, Q., Raczek, I., Jacob, D.E., Stracke, A., Birbaum, K., Frick, D.A., Günther, D. and Enzweiler, J. (2011) Determination of

Reference Values for NIST SRM 610–617 Glasses Following ISO Guidelines. Geostandards and Geoanalytical Research 35, 397-429.

Jaccard, S.L. and Galbraith, E. (2012) Large climate-driven changes of oceanic oxygen concentrations during the last deglaciation. Nature Geoscience 5, 151-156.

Key, R.M., Kozyr, A., Sabine, C., Lee, K., Wanninkhof, R., Bullister, J.L., Feely, R.A., Millero, F.J., Mordy, C. and Peng, T.-H. (2004) A global ocean carbon climatology: Results from the Global Data Analysis Project (GLODAP). Global Biogeochem. Cycles 18, 1-23.

Klinkhammer, G. and Palmer, M.R. (1991) Uranium in the oceans: Where it goes and why. Geochimica et Cosmochimica Acta 55, 1799-1806.

McCorkle, D.C. and Emerson, S. (1988) The relationship between pore water carbon isotopic composition and bottom water oxygen concentration. Geochimica et Cosmochimica Acta 52, 1169-1178.

Misra, S., Greaves, M., Owen, R., Kerr, J., Elmore, A.C. and Elderfield, H. (2014) Determination of B/Ca of natural carbonates by HR-ICP-MS. Geochem. Geophys. Geosys. 15, 1617-1628.

Oka, A., Hasumi, H., Obata, H., Gamo, T. and Yamanaka, Y. (2009) Study on vertical profiles of rare earth elements by using an ocean general circulation model. Global Biogeochem. Cycles 23, GB4025.

Osborne, A.H., Hathorne, E.C., Schijf, J., Plancherel, Y., Böning, P. and Frank, M. (2017) The potential of sedimentary foraminiferal rare earth element patterns to trace water masses in the past. Geochem. Geophys. Geosys. 18, 1550-1568.

Palmer, M.R. and Elderfield, H. (1985) Variations in the Nd isotopic composition of foraminifera from Atlantic Ocean sediments. Earth Planet. Sci. Lett. 73, 299-305.

Pourmand, A., Dauphas, N. and Ireland, T.J. (2012) A novel extraction chromatography and MC-ICP-MS technique for rapid analysis of REE, Sc and Y: Revising CI-chondrite and Post-Archean Australian Shale

(PAAS) abundances. Chemical Geology 291, 38-54.

Roberts, N.L., Piotrowski, A.M., Elderfield, H., Eglinton, T.I. and Lomas, M.W. (2012) Rare earth element association with foraminifera. Geochimica et Cosmochimica Acta 94, 57-71.

Roberts, N.L., Piotrowski, A.M., McManus, J.F. and Keigwin, L.D. (2010) Synchronous deglacial overturning and water mass source changes. Science 327, 75-78.

Rousseau, T.C.C., Sonke, J.E., Chmeleff, J., Candaudap, F., Lacan, F., Boaventura, G., Seyler, P. and Jeandel, C. (2013) Rare earth element analysis in natural waters by multiple isotope dilution - sector field ICP-MS. Journal of Analytical Atomic Spectrometry 28, 573.

Sholkovitz, E.R., Landing, W.M. and Lewis, B.L. (1994) Ocean particle chemistry: The fractionation of rare earth elements between suspended particles and seawater. Geochimica et Cosmochimica Acta 58, 1567-1579.

Skinner, L.C., Fallon, S., Waelbroeck, C., Michel, E. and Barker, S. (2010) Ventilation of the deep Southern Ocean and deglacial CO2 rise. Science 328, 1147-1151.

Skinner, L.C., Primeau, F., Freeman, E., de la Fuente, M., Goodwin, P., Gottschalk, J., Huang, E., McCave, I.N., Noble, T. and Scrivner, A.E. (2017) Radiocarbon constraints on the 'glacial' ocean circulation and its impact on atmospheric CO2. Nature Communications.

Skinner, L.C., Scrivner, A., Vance, D., Barker, S., Fallon, S. and Waelbroeck, C. (2013) North Atlantic versus Southern Ocean contributions to a deglacial surge in deep ocean ventilation. Geology 41, 667-670.

Skinner, L.C., Waelbroeck, C., Scrivner, A. and Fallon, S. (2014) Radiocarbon evidence for alternating northern and southern sources of ventilation of the deep Atlantic carbon pool during the last deglaciation. Proceedings of the National Academy of Sciences 111, 5480–5484.

Tachikawa, K., Toyofuku, T., Basile-Doelsch, I. and Delhaye, T. (2013) Microscale neodymium distribution in sedimentary planktonic foraminiferal tests and associated mineral phases. Geochimica et Cosmochimica Acta 100, 11-23.

Tanner, S.D., Baranov, V.I. and Bandura, D.R. (2002) Reaction cells and collision cells for ICP-MS: a tutorial review Spectrochimica Acta Part B-Atomic Spectroscopy 57, 1361–1452.

Wilson, D.J., Piotrowski, A.M., Galy, A. and Clegg, J.A. (2013) Reactivity of neodymium carriers in deep sea sediments: Implications for boundary exchange and paleoceanography. Geochimica et Cosmochimica Acta 109, 197-221.

Zheng, X., Plancherel, Y., Saito, M.A., Scott, P. and Henderson, G.M. (2016) Rare earth elements (REEs) in the tropical South Atlantic and quantitative deconvolution of their non-conservative behaviour. Geochimica et Cosmochimica Acta 177, 217-237.

Zheng, X.-Y., Yang, J. and Henderson, G.M. (2014) A robust procedure for high-precision determination of rare earth element concentrations in seawater. Geostand. Geoanal. Res. 39, 277-292.

Figure 1.

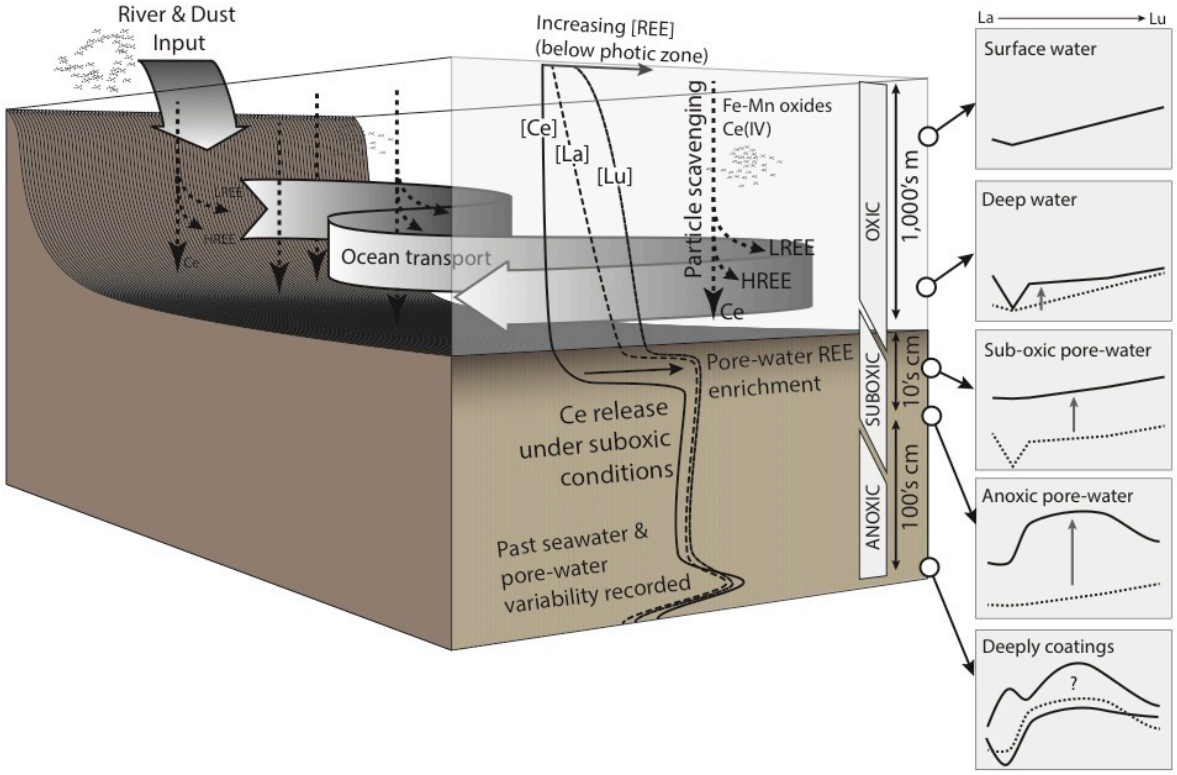

Figure 1. Schematic of REE cycling in the marine and shallow sedimentary environment, after (Haley et al., 2004). Insets at right show typical PAAS-normalised REE profiles for different locations in the water column/sediment, where dashed lines indicate the profile inherited from shallower in the sediment column, and solid lines indicate the profile that develops at that depth. 'Deep coatings' refers to surface enrichments on deeply buried foraminifera. Key processes in this context include the interplay between particle scavenging and transport in the water column, and between particulate oxide reduction and organic carbon respiration in sediments.

Figure 2.

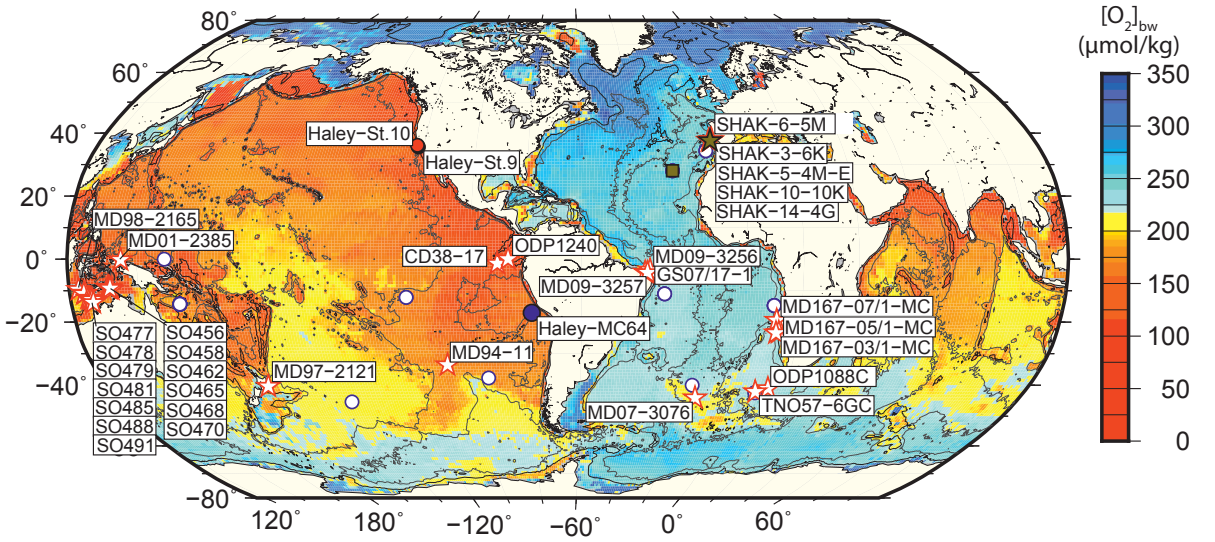

Figure 2. Location of sediment and seawater samples referred to in this study, plotted on top of bottom water oxygen field (Garcia et al., 2014). Core locations are indicated by open stars and site names are labelled, published seawater data from proximal locations (compiled by (Osborne et al., 2017)) are indicated by open circles. Filled circles indicate the locations of additional published seawater, pore-water and foraminifer REE data referred to in this study (Greaves, 1988; Haley et al., 2004; Haley et al., 2005). The filled star indicates the location of 'multi-core' SHAK-6-5M.

Figure 3.

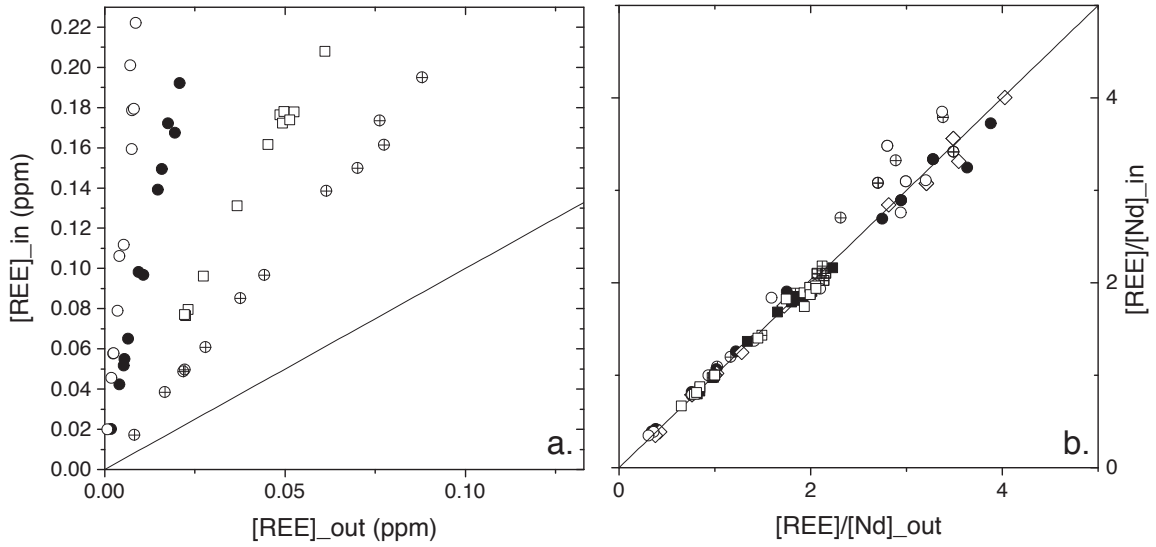

Figure 3. Comparison of LA-ICPMS REE analyses performed on the interior and exterior surfaces of planktonic foraminifer shells ('mechanically cleaned' and pre-ablated to remove adherent detrital material/clays). Different symbols denote different samples (i.e. separate collections of co-deposited foraminifer shell fragments). REE distributions are coherent between the interior and exterior surfaces despite much greater REE enrichment on interior surfaces. Plot (a) compares absolute REE concentrations on interior and exterior surfaces from the same sample (though not identical shell fragments), while plot (b) compares REE concentrations on interior and exterior surface normalized to [Nd] for the purpose of illustration. Note that the greatest scatter in (b) coincides with the occurrence of very low, and therefore less reproducible $[Nd]_{out}$.

Figure 4.

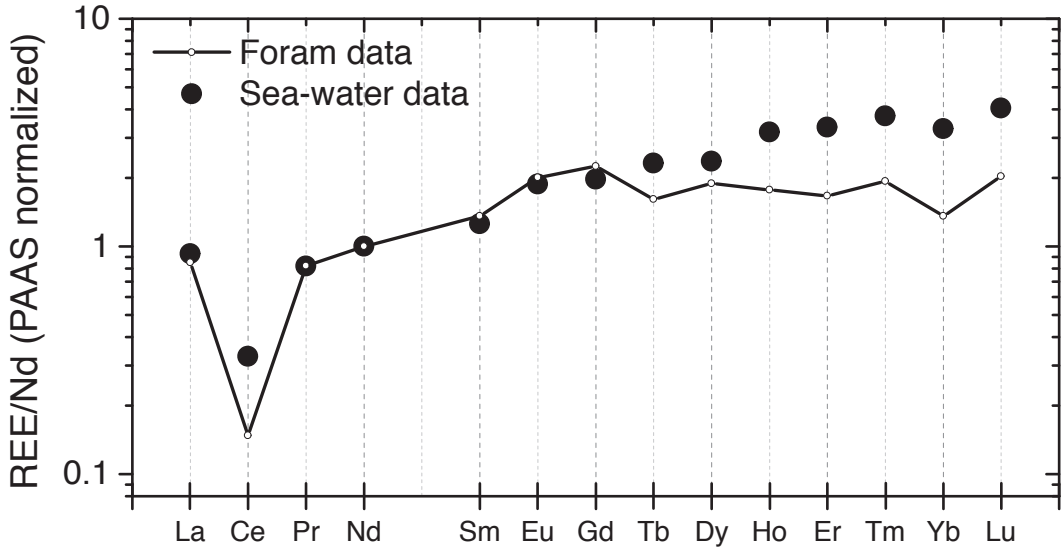

Figure 4. Comparison of the REE distribution in seawater obtained from just above the sediment-water interface of multi-core SHAK-6-5M (solid symbols) with the REE distribution in foraminifer 'coatings' (solid line), measured by LA-ICPMS on sedimentary core-top material from just below the sediment-water interface (0-1cm). Data are PAAS-normalized (Pourmand et al., 2012), with each REE concentration then expressed relative to Nd for ease of comparison between seawater/foraminifer values. The foraminifer data displays a characteristic 'seawater signature', albeit with an apparent depletion in HREE as compared to seawater as typically observed in authigenic REE data (Osborne et al., 2017).

Figure 5.

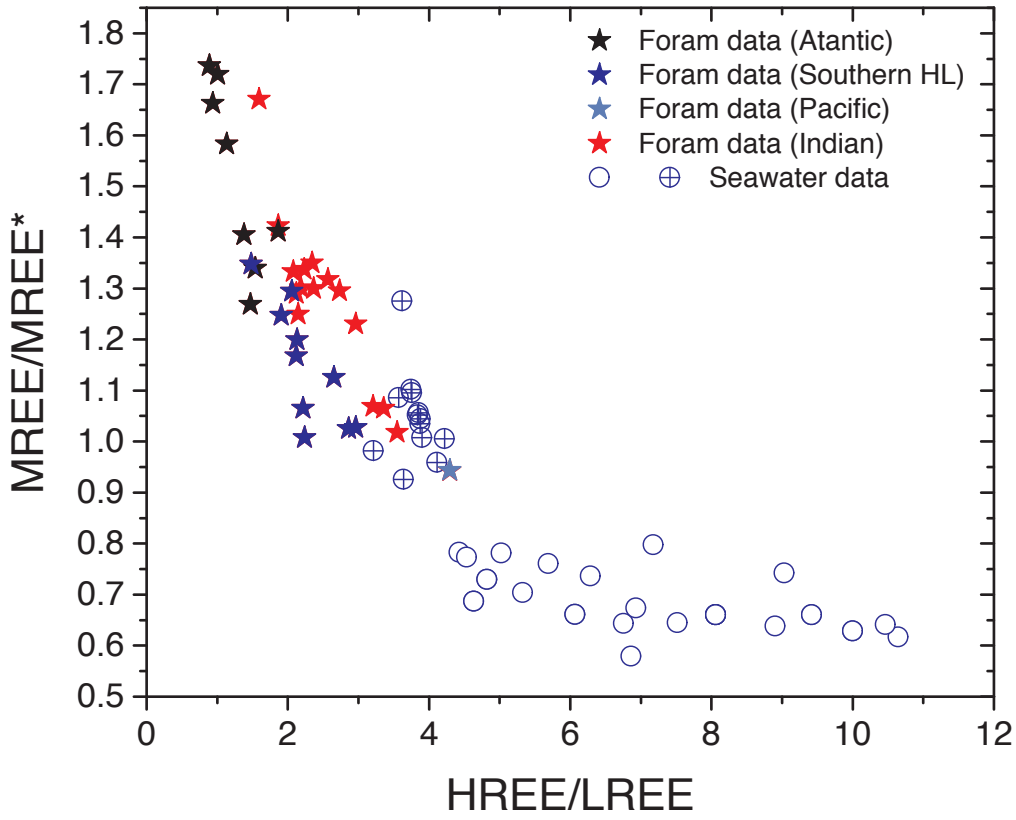

Figure 5. Comparison of HREE/LREE and MREE/MREE* measured in foraminifer 'coatings' (filled stars) from a global core-top array (samples typically from 0-1, 1-2 or 2-3cm depth), with seawater data from nearby locations. Seawater data are drawn from the compilation of (Osborne et al., 2017) at nearest possible locations to core-top sites (open circles), as well as a profile from the Iberian Margin (Greaves, 1988) (site SH6-1B79, 34°40'N, 09°20'W; crossed circles). Note that HREE/LREE and MREE/MREE* for all data sources have been calculated based on the definitions given in the text after normalisation to PAAS (Pourmand et al., 2012).

Figure 6.

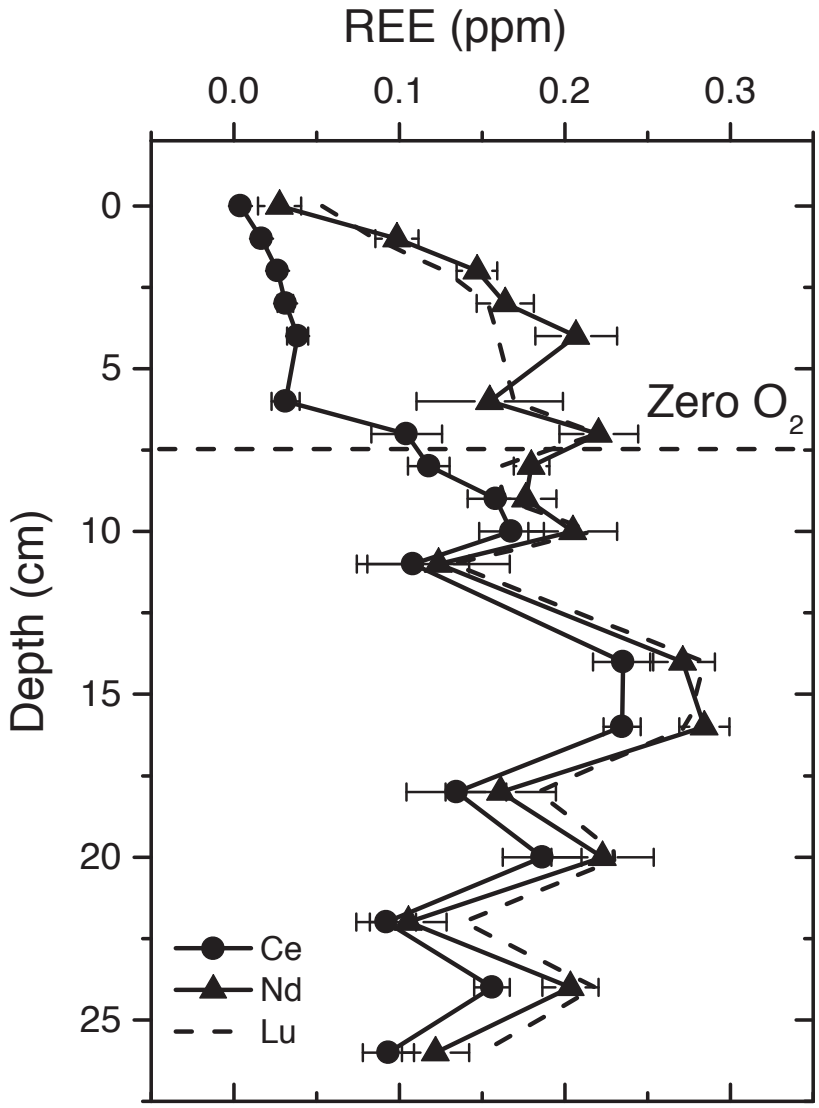

Figure 6. REE concentrations measured by LA-ICPMS in foraminifer 'coatings' in multi-core SHAK-6-5M; Lu, Nd, and Ce are shown for illustrative purposes (error bars indicate 1SD). In general REE concentrations increase rapidly across the first few centimetres of sediment, with the exception of Ce which only increases once sub-oxic/anoxic pore-water conditions occur.

Figure 7.

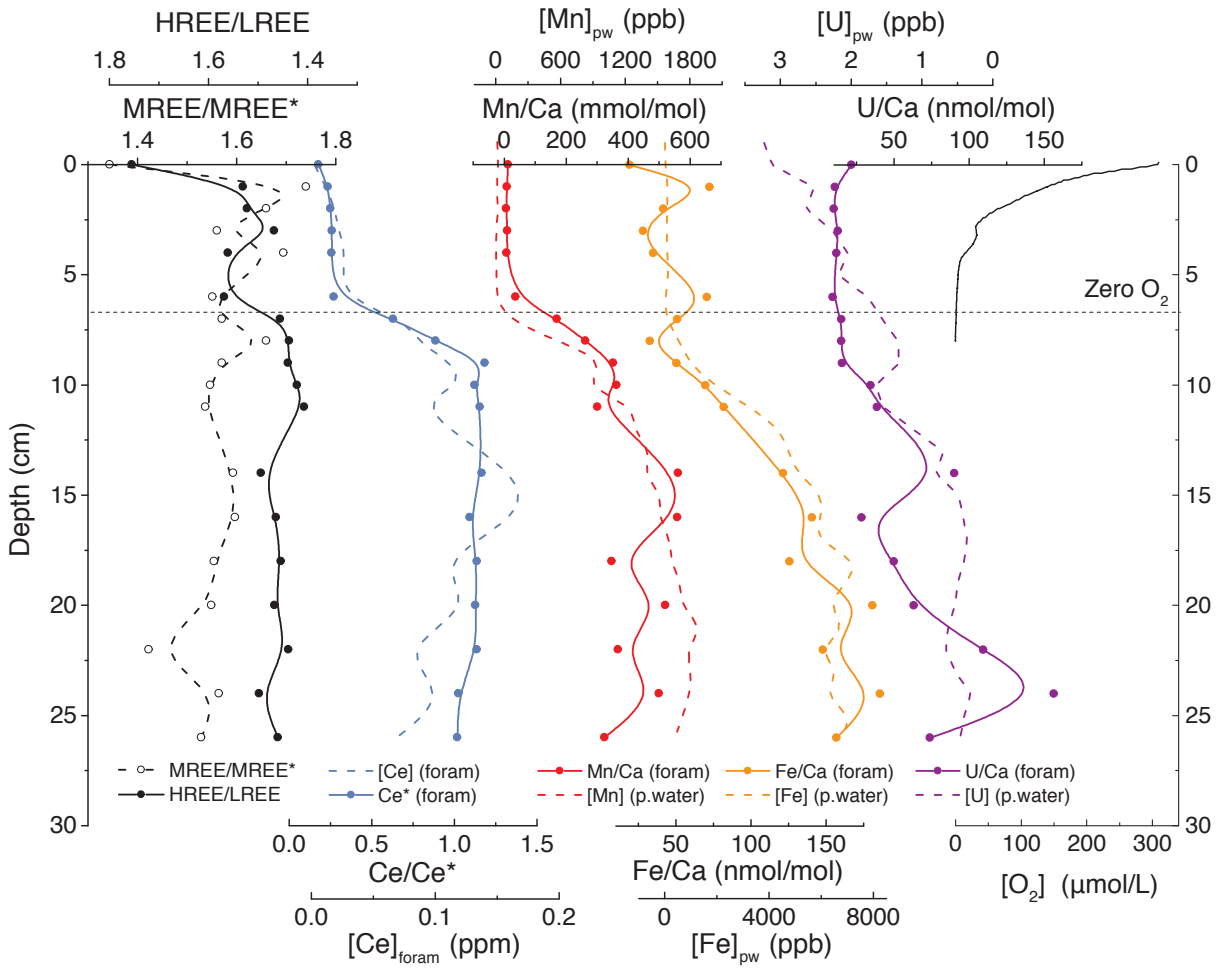

Figure 7. REEfs and pore-water data from multi-core SHAK-6-5M, from the Iberian Margin. Note reversed scale for pore-water [U], which varies inversely compared to foraminifer 'coating' U/Ca, unlike Mn/Ca and Fe/Ca which track Mn and Fe concentrations in pore-water. The horizontal dashed line indicates the depth of zero measureable oxygen, measured *in situ*.

Figure 8.

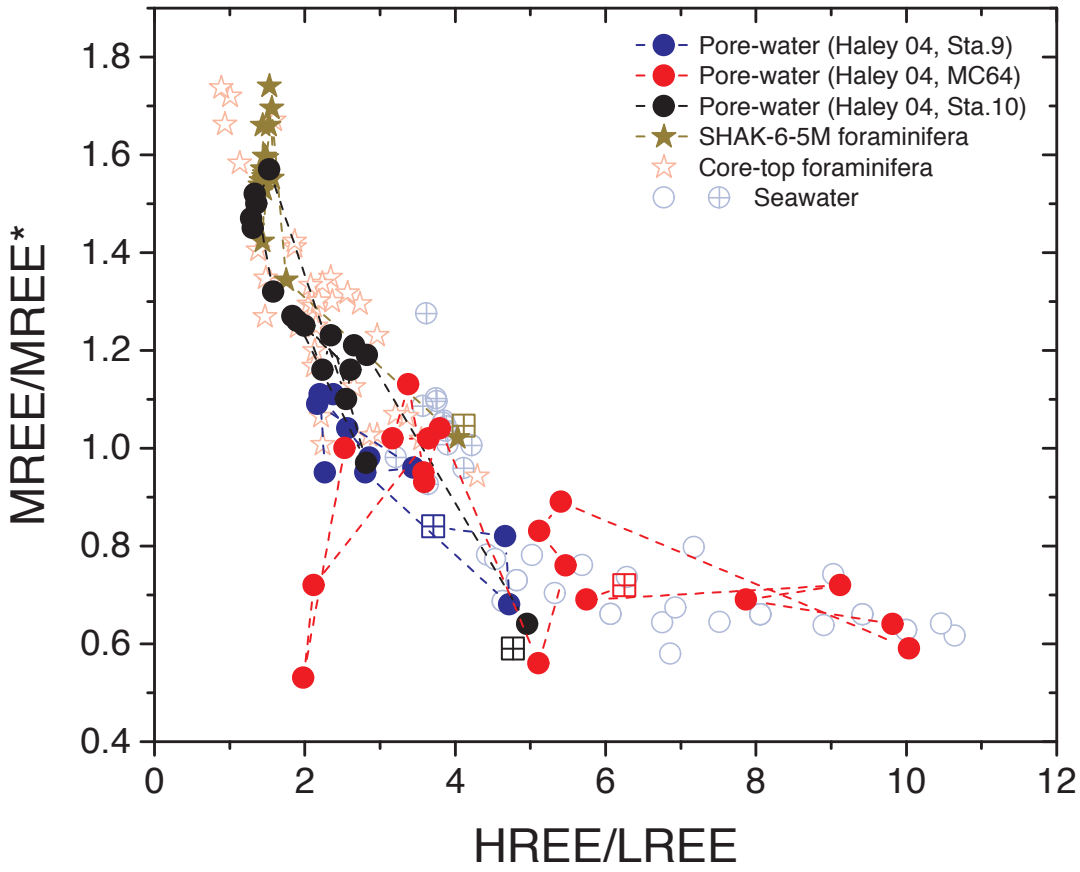

Figure 8. Comparison of published pore-water REE data from the SE Pacific (Haley et al., 2004) and authigenic 'coating' REE data from near the sediment-water interface (this study), illustrating a down-core trend from the 'seawater regime' (bottom right) to the 'authigenic regime' (top left) at each location. Open circles indicate seawater data (as per Figure 5); open stars indicate globally distributed core-top foraminifer REEfs data (this study); filled circles indicate pore-water data (Haley et al., 2004); filled stars indicate down-core foraminifer REEfs data from site SHAK-6-5M (this study). Large crossed squares indicate seawater data from above the sediment-water interface at each location (either from (Haley et al., 2004) or from this study – see Figure 4). Pore-water compositions generally evolve away from seawater values (indicated by crossed squares) toward the top-left with deeper burial; REEfs data from SHAK-6-5M mimic this same trend.

Figure 9.

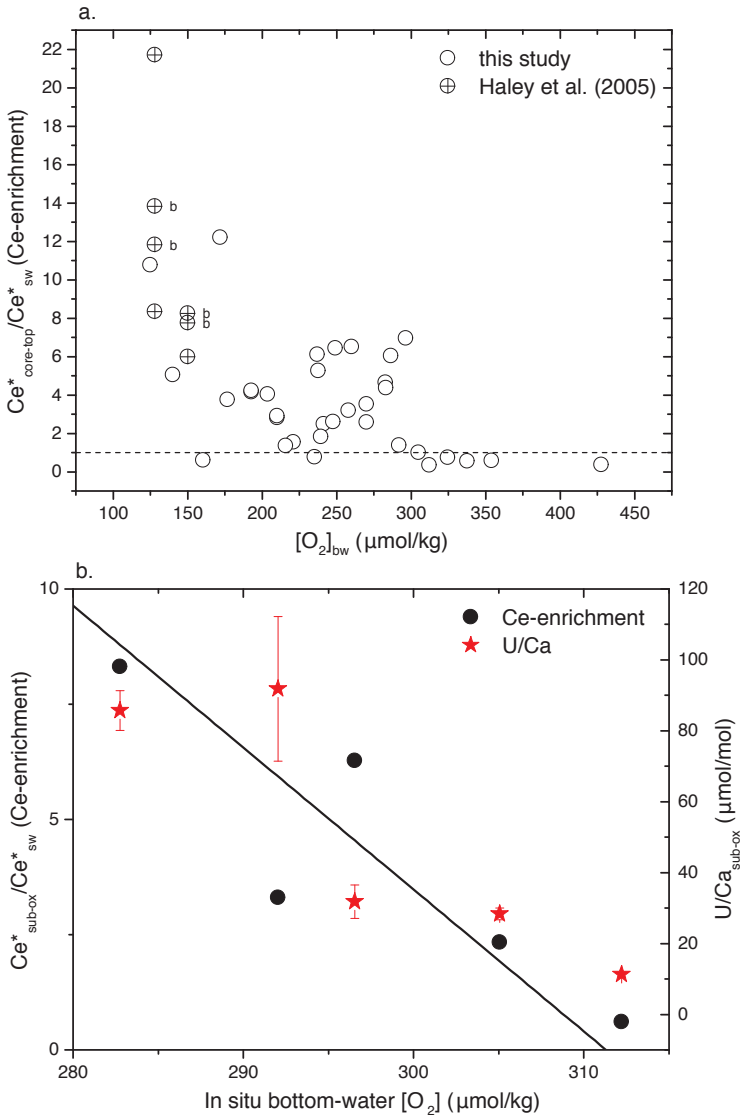

Figure 9. Comparison of bottom water oxygen concentrations *versus* Cerium and Uranium enrichment on the inner surfaces of recently deposited foraminifer shells: **a.** Ce-enrichment in sedimentary core-top planktonic foraminifer 'coatings' (defined as $Ce^*_{core\text{-}top}/Ce^*_{seawater}$, using published seawater values taken from nearby locations) compared with approximate bottom-water oxygen concentrations interpolated from the GLODAP database (Key et al., 2004) at the core-top locations, showing a tendency for greater enrichment relative to seawater values under lower oxygenation. Data from (Haley et al., 2005) are shown by crossed circles, where 'b' indicates measurements on benthic foraminifera. **b.** Ce-enrichment and U/Ca measured in sub-modern foraminifera that have already passed into sub-oxic conditions (14-16cm below the sediment-water interface), compared with *in situ* bottom-water oxygen concentrations measured just above the sediment-water interface. Error bars indicate 2SE estimates (visible only for U/Ca).

Figure 10.

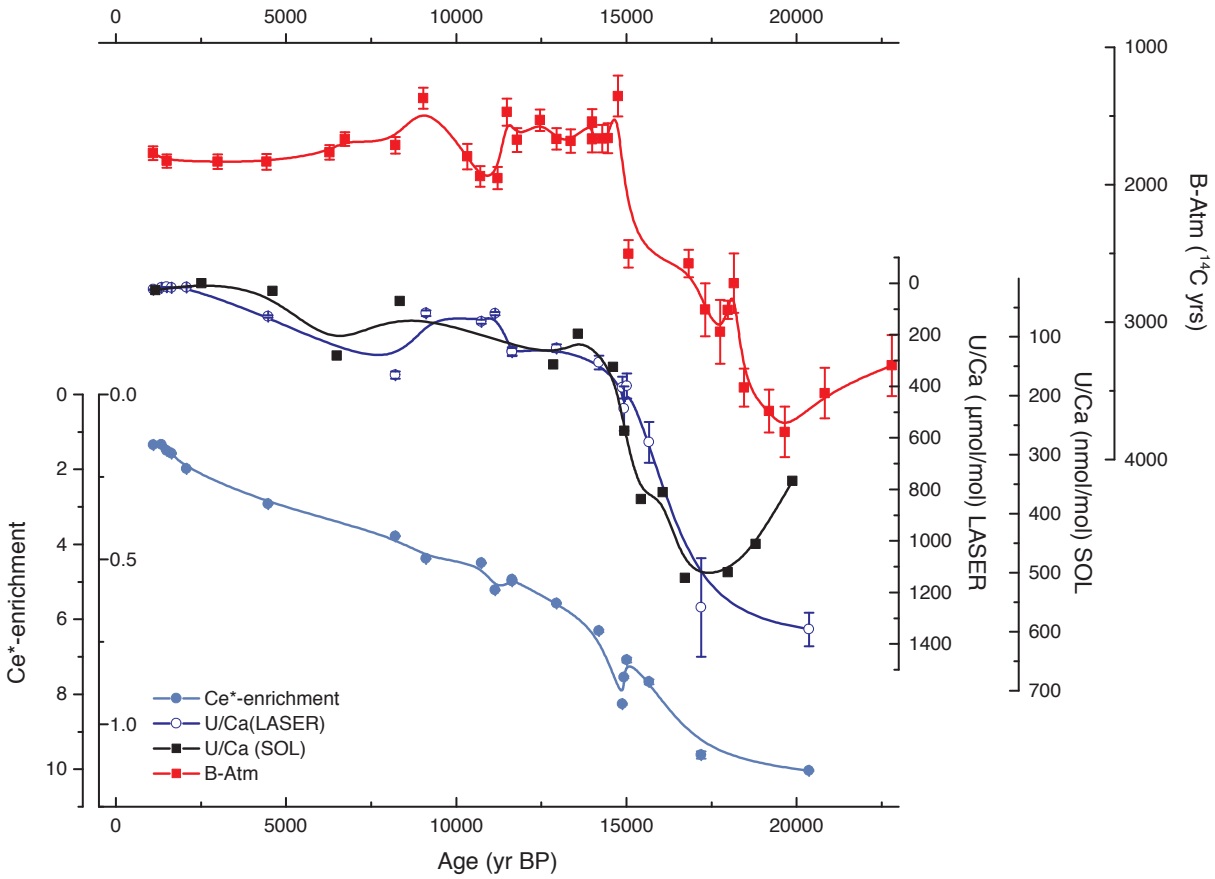

Figure 10. Down-core records from MD07-3076 (Sub-Antarctic Atlantic). Previously published 'radiocarbon ventilation age' data (Skinner et al., 2014) (red squares and solid line) and U/Ca data obtained by solution-based ICPMS methods (Gottschalk et al., 2016) (black squares and solid line), are compared with Ce-enrichment and U/Ca data obtained by LA-ICPMS analysis (this study; open blue circles and filled light blue circles, respectively). Outer and inner y-axes on bottom plot indicate the Ce-enrichment (defined as down-core Ce/Ce* divided by modern seawater Ce/Ce*) and the Ce/Ce* values respectively. Errors indicate 2 SE (not always visible).

Figure 11.

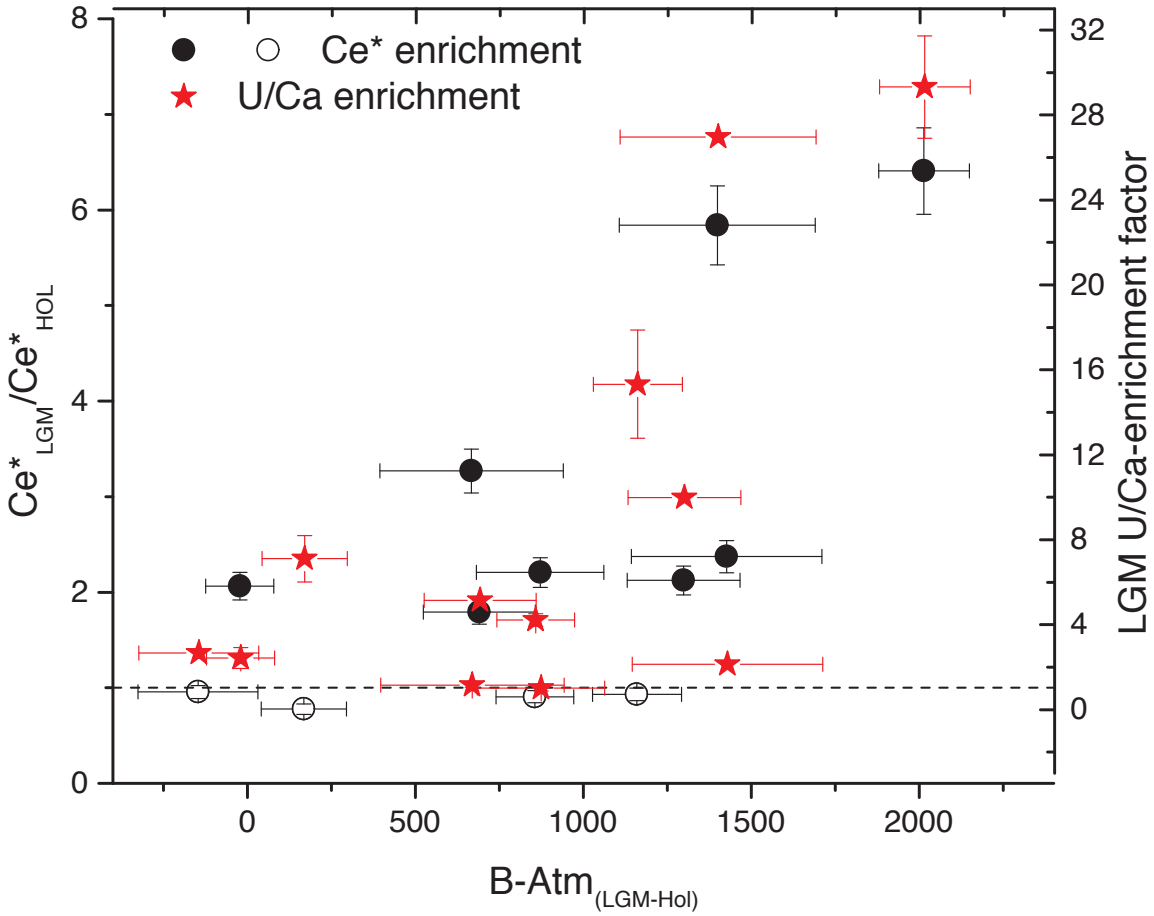

Figure 11. Comparison of Last Glacial Maximum (LGM) Ce-enrichment (circles) and U/Ca-enrichment (stars), both expressed as LGM vs. Holocene/core-top ratios, with co-registered deep-water 'radiocarbon ventilation ages' (Skinner et al., 2017), expressed as benthic-atmospheric (B-Atm) radiocarbon age offsets. Horizontal line indicates a value of 1, and pen circles indicate LGM Ce-enrichment values <1, indicating a lower Ce/Ce* recorded in LGM sediments as compared to the late Holocene/core-top, possibly due to the lack of any anoxic diagenesis occurring at these sites, as well as a change in seawater Ce/Ce*. Errors indicate 2 SE.

SUPPLEMENTARY FIGURE S1

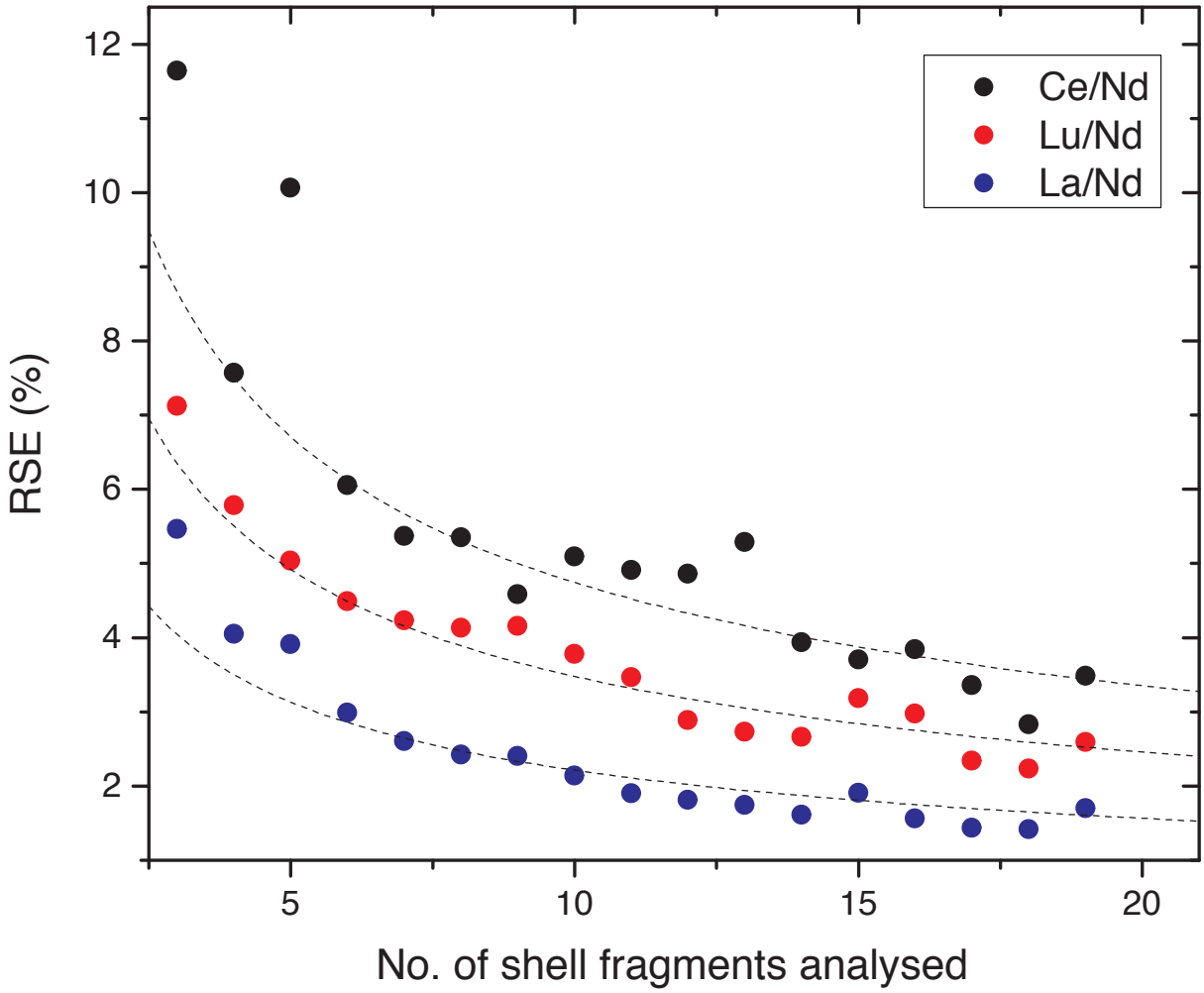

Figure S1. Illustration of evolving relative standard error (% RSE) as a function of the number of foraminifer shell fragments analysed (i.e. number of ablations), for three illustrative elemental ratios. Dashed lines indicate hypothetical relations for %RSE as a function of observation number for constant measurement standard deviations close to ~10% RSD.